Structural study of Al2O3-Na2O-CaO-P2O5 bioactive glasses as a function of aluminium content

J. M. Smith, S. P. King, E. R. Barney, J. V. Hanna, R. J. Newport et al.

Citation: J. Chem. Phys. **138**, 034501 (2013); doi: 10.1063/1.4774330
View online: http://dx.doi.org/10.1063/1.4774330
View Table of Contents: http://jcp.aip.org/resource/1/JCPSA6/v138/i3
Published by the AIP Publishing LLC.

Structural study of Al_2O_3-Na_2O-CaO-P_2O_5 bioactive glasses as a function of aluminium content

J. M. Smith,[1] S. P. King,[2] E. R. Barney,[3] J. V. Hanna,[2] R. J. Newport,[1] and D. M. Pickup[1,a)]
[1]*School of Physical Sciences, University of Kent, Canterbury CT2 7NH, United Kingdom*
[2]*Department of Physics, University of Warwick, Coventry CV4 7AL, United Kingdom*
[3]*Electrical Systems and Optics Research Division, Faculty of Engineering, University of Nottingham, Nottingham NG7 2RD, United Kingdom*

(Received 1 November 2012; accepted 20 December 2012; published online 15 January 2013)

Calcium phosphate based biomaterials are extensively used in the context of tissue engineering: small changes in composition can lead to significant changes in properties allowing their use in a wide range of applications. Samples of composition $(Al_2O_3)_x(Na_2O)_{0.11-x}(CaO)_{0.445}(P_2O_5)_{0.445}$, where x = 0, 0.03, 0.05, and 0.08, were prepared by melt quenching. The atomic-scale structure has been studied using neutron diffraction and solid state ^{27}Al MAS NMR, and these data have been rationalised with the determined density of the final glass product. With increasing aluminium concentration the density increases initially, but beyond about 3 mol. % Al_2O_3 the density starts to decrease. Neutron diffraction data show a concomitant change in the aluminium speciation, which is confirmed by ^{27}Al MAS NMR studies. The NMR data reveal that aluminium is present in 4, 5, and 6-fold coordination and that the relative concentrations of these environments change with increasing aluminium concentration. Materials containing aluminium in 6-fold coordination tend to have higher densities than analogous materials with the aluminium found in 4-fold coordination. Thus, the density changes may readily be explained in terms of an increase in the relative concentration of 4-coordinated aluminium at the expense of 6-fold aluminium as the Al_2O_3 content is increased beyond 3 mol. %.
 [http://dx.doi.org/10.1063/1.4774330]

I. INTRODUCTION

Phosphate based glasses containing sodium and calcium are very adaptable materials; small changes in their composition can lead to significant changes to key properties such as the solubility.[1,2] Such glasses have high thermal coefficients and a relatively low melting temperature, making them easy to form as glassy materials.[3] The wide range in properties that can be achieved and the ease of glass formation over a wide range of compositions offers the potential of being able to tailor them to the particular requirements of a diverse range applications including seals,[3] laser systems,[4] and biomaterials, for example.[2,5]

Biomaterials are materials which may have a tissue-regenerative effect; bioactive glass is one such material.[6] When bioactive glasses are in contact with physiological fluid they begin to break down. The dissolution products generated stimulate the up-regulation of bone-forming cells while the remaining material acts as a scaffold for the cells to attach to so that the bone can grow.[6] Phosphate based biomaterials have an advantage in that they are closer in composition to natural bone[5,7,8] and the rate of dissolution can more easily be tailored to the end application;[2,5] for example, coatings on long term implants require a lower dissolution rate but require the same level of bioactivity.[8] The addition of a small amount of aluminium reduces the dissolution rate while increasing the bioactivity; the density is also increased.[8] However, adding larger quantities of aluminium has the effect of reducing both the bioactivity and density.[9]

As a consequence of the variety of current and potential applications, phosphate based glassy materials have been studied using a range of techniques including computer modelling,[1] Fourier transform infrared spectroscopy,[2,8] Raman spectroscopy,[10] solid state MAS NMR spectroscopy,[11] and both x-ray and neutron diffraction.[1,12,13] The structure of aluminium containing phosphate based glasses has also been extensively studied using NMR spectroscopy in addition to other techniques.[10,14–17] Previous ^{27}Al MAS NMR studies have shown the aluminium to be present in 4-, 5-, and 6-fold coordination.[17–20] One such study on sodium aluminophosphates demonstrated that at low concentrations, aluminium adopts a 6-fold coordinated environment.[20] However, as the concentration of Al_2O_3 is increased above ~5 mol. %, the average aluminium coordination number decreases as 4 and 5-fold environments are formed at the expense of aluminium in octahedral units. However, the fraction of 5-fold aluminium is always less that ~25%, regardless of the aluminium concentration.

To study to effect of aluminium on the structure of phosphate glasses, four samples of composition $(Al_2O_3)_x(Na_2O)_{0.11-x}(CaO)_{0.445}(P_2O_5)_{0.445}$, where x = 0, 0.03, 0.05, or 0.08, were prepared by melt quenching. The densities of these samples were measured, and their structures were studied using neutron diffraction and ^{27}Al MAS NMR spectroscopy. The data were analysed with the aim of attempting to explain the pronounced bioactivity and density trends on the basis of the local aluminium

a)Author to whom correspondence should be addressed. Electronic mail: d.m.pickup@kent.ac.uk.

environment and any affect it may have on the overall glass network.

II. EXPERIMENTAL

A. Sample preparation

The required amounts of calcium phosphate dibasic, aluminium oxide, ammonium phosphate, and sodium carbonate were mixed to obtain a series of glasses of composition $(Al_2O_3)_x(Na_2O)_{0.11-x}(CaO)_{0.445}(P_2O_5)_{0.445}$, where x = 0, 0.03, 0.05, or 0.08. The precursor chemicals were purchased from Sigma Aldrich and were all 99.9% pure. The glass samples were made using a conventional melt quench process: the mix was heated from room temperature to 1250 °C at a rate of at 10 °C/min; the final temperature was held for 2 h before the molten glass was poured into graphite moulds pre-heated to 350 °C. The solid samples were annealed overnight in an oven at 450 °C and subsequently cooled to room temperature at 1 °C/min.

B. Density measurements

The density of each glass sample was measured using a Micromeritics® Accupyc1340 pycnometer, which utilizes Archimedes' Principle using helium gas as the fluid.

C. Neutron scattering

The neutron diffraction data presented herein were collected on the General Materials (GEM) time-of-flight diffractometer on the International Science Information Service spallation neutron source at the Rutherford Appleton Laboratory, UK.[21] The samples were contained in vanadium cans of internal diameter 8.3 mm and wall thickness 0.025 mm; a vanadium rod of diameter 8 mm was used to provide quantitative normalisation to the data. Data were collected from the empty instrument, empty V container, and the V rod in addition to each of the samples; data were collected over a wide dynamic range (scattering vector Q from 0.5 to 60 $Å^{-1}$, where $Q = 4\pi\sin\theta/\lambda$).

The initial stage of analysis of data from an amorphous material involves the removal of the various sources of background scattering (from the instrument itself and from the container), normalization, correction for absorption, inelastic and multiple scattering, and subtraction of the self-scattering term.[21] The resultant scattered intensity, $S(Q) - 1$, can reveal structural information by Fourier transformation to yield the pair distribution function:

$$T(r) = T^0(r) + \frac{\pi}{2}\int_0^\infty Q\,[S(Q) - 1]\,M(Q)\sin(Qr)dQ, \tag{1}$$

where

$$T^o(r) = 4\pi r\rho_o, \tag{2}$$

r is the atomic separation between pairs of atoms, ρ_o is the macroscopic number density, and $M(Q)$ is a window function necessitated by the finite maximum experimentally attainable value of Q; for the work presented herein, the window function used was a Lorch function.[22]

Structural information can be obtained from the diffraction data by simulating the Q-space data and converting the results to r-space by Fourier transformation to allow comparison with the experimentally determined correlation function.[23] The Q-space simulation is generated using the following equation:

$$p(Q)_{ij} = \frac{N_{ij}w_{ij}}{c_j}\frac{\sin QR_{ij}}{QR_{ij}}\exp\left[\frac{-Q^2\sigma_{ij}^2}{2}\right], \tag{3}$$

where $p(Q)_{ij}$ is the pair function in reciprocal space, N_{ij}, R_{ij}, and σ_{ij} are the coordination number, atomic separation, and disorder parameter, respectively, of atom i with respect to j, c_j is the concentration of atom j, and w_{ij} is the weighting factor, given by

$$w_{ij} = \frac{2c_ic_jb_ib_j}{\left(\sum_i c_ib_i\right)^2} \quad \text{if } i \neq j, \tag{4}$$

$$w_{ij} = \frac{c_i^2b_i^2}{\left(\sum_i c_ib_i\right)^2} \quad \text{if } i = j, \tag{5}$$

where b represents the coherent neutron scattering length. Due to sodium and calcium having similar ionic radii, of 0.99 and 0.95 Å, respectively, there is little difference in the atomic separations in the Ca–O (2.34 Å) and Na–O (2.33 Å) correlations.[24] Therefore, to simplify the fitting process, a generic metal cation has been used which has the average scattering length, weighted by the concentration of the two elements.

D. ^{27}Al MAS NMR measurements

Solid State ^{27}Al MAS NMR measurements were performed at ambient temperatures using Bruker DSX-400 (9.4 T) and Bruker Avance II-600 (14.1 T) spectrometers. All ^{27}Al data were acquired using Bruker 3.2 mm dual channel (HX) probes in which MAS frequencies of 20 kHz were attained for each measurement. Single pulse experiments were employed for all data acquisition, where a relaxation delay of 5 s and a tip angle of $\pi/12$ were used to ensure that quantitative estimates of all aluminium speciation had been achieved. All ^{27}Al spectra were referenced to the IUPAC primary reference of $Al(NO_3)_3$ (1.1 M in D_2O) via a secondary reference of yttrium aluminium garnet (YAG) in which the six coordinate resonance is a known shift of 0.7 ppm. The analysis of all ^{27}Al MAS NMR data at each B_0 field was undertaken using the QUADFIT simulation program.[25]

III. RESULTS

The densities of the four glass samples measured by helium pycnometery follow the trend previously described in the literature.[9] This unusual density trend is shown in Figure 1. Initial substitution of a few mol. % of Na_2O by Al_2O_3 causes the density to increase but further substitution results in the density decreasing.

Figures 2–4 show the neutron diffraction data from the three Al containing samples. Both Q-space scattering inten-

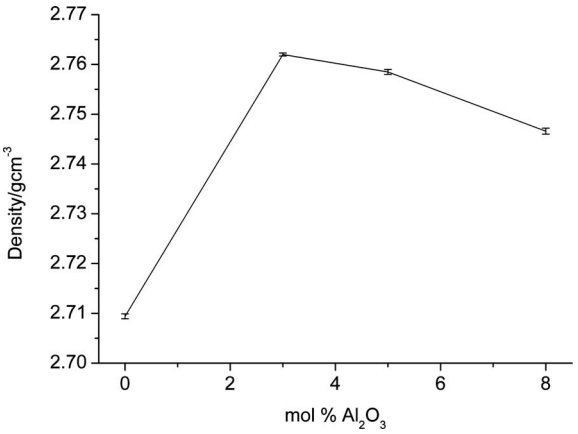

FIG. 1. Glass density as a function of Al_2O_3 concentration using helium pycnometry.

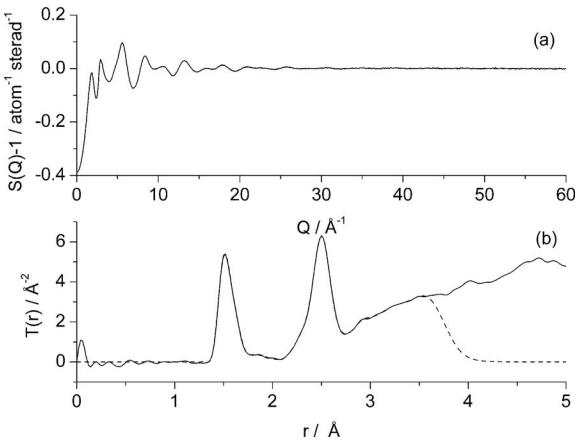

FIG. 3. Neutron diffraction data from the 5 mol. % Al_2O_3 sample (a) *Q*-space data; (b) *r*-space pair distribution factor, $T(r)$ (solid line) and the fit (dotted line).

sity and *r*-space pair distribution functions are shown together with *r*-space fit obtained by the method described previously. The structural parameters obtained from the fitting process are given in Table I. The starting parameters used in the fitting process have been chosen on the basis of previous studies[1,12] and the chemical database of inorganic crystals.[26–34]

The relative concentrations of the various aluminium environments were determined both from the MAS NMR data and corresponding neutron diffraction data. From the ^{27}Al MAS NMR spectra for each sample acquired at external B_0 field strengths of 9.4 and 14.1 T (see Figure 5), it is readily observed that aluminium speciation is described by 4-, 5-, and 6-fold coordinated oxo environments in each of these glass systems. The impurity visible in the 8 mol. % sample in Figure 5 is likely to be a crystal phase present in low concentration. The fact that this phase is not observed by neutron diffraction suggests that it is present in discrete domains which are small enough to broaden any Bragg peaks beyond the detection limit.

The dual-field ^{27}Al MAS NMR data for each sample were simulated using the QUADFIT simulation program which elucidates the isotropic chemical shift (δ_{iso}), quadrupole coupling constant (C_Q), distributions in quadrupole parameters, and integrated intensity from each spectrum.[25] This analysis was performed iteratively between the dataset from each field until a consistency of <5% in the residual-sum-of-squares error was achieved; the resultant simulations pertaining to these analyses are also shown in Figure 5 and the numerical results are summarised in Table II.

From the neutron diffraction data a quantitative analysis was achieved by first assigning the peaks in the pair distribution function at ∼1.7, ∼1.8, and ∼1.9 Å to aluminium in 4-, 5-, and 6-fold coordination environments, respectively.[35] The proportions of each aluminium environment present were then calculated from the relative areas of these three peaks. A comparison of the results from the two techniques is shown in Figure 6.

It should be noted that NMR is element specific and is therefore much more sensitive to the aluminium environment at low concentrations. At the lowest concentration of Al_2O_3, the aluminium is predominantly 6 coordinate with respect to oxygen. However, for increasing Al_2O_3 content an increase in the relative concentration of 4-fold aluminium at the expense of 6-fold aluminium is observed. The concentration of 5-fold

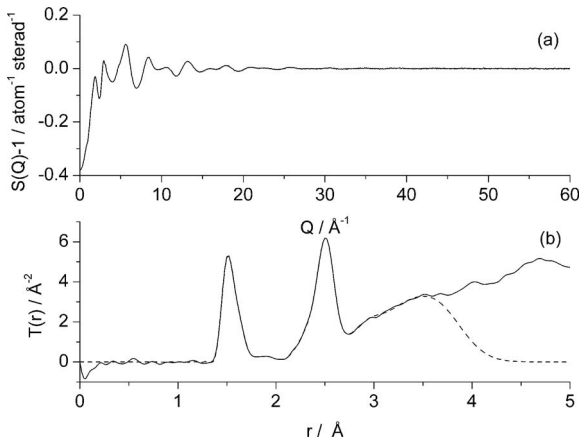

FIG. 2. Neutron diffraction data from the 3 mol. % Al_2O_3 sample (a) *Q*-space data; (b) *r*-space pair distribution factor, $T(r)$ (solid line) and the fit (dotted line).

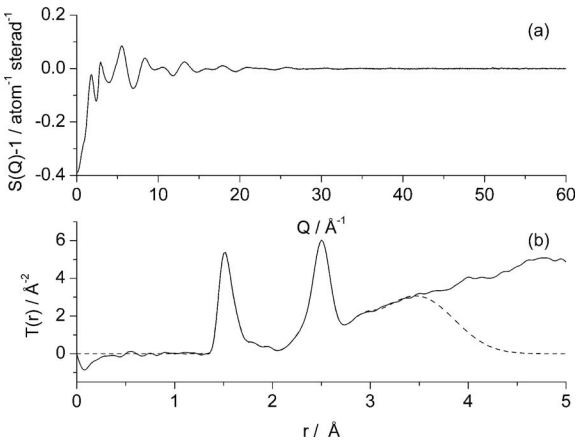

FIG. 4. Neutron diffraction data from the 8 mol. % Al_2O_3 sample (a) *Q*-space data; (b) *r*-space pair distribution factor, $T(r)$ (solid line) and the fit (dotted line).

TABLE I. Structural parameters obtained from simulation of the neutron diffraction data. Note that *M* denotes the generic metal cation, BO is a bridging oxygen, and NBO is a non-bridging oxygen. The errors are reasonably estimated as ±0.02 Å in *R*, ±15% in *N*, and ±0.01 Å in σ.

Sample	Density (g cm^{-3})	Correlation	*R* (Å)	*N*	σ (Å)
$(CaO)_{0.445}(P_2O_5)_{0.445}(Na_2O)_{0.11}$	2.7094(5)	P–NBO	1.50	2.2	0.042
		P–BO	1.60	1.6	0.062
		M–O	2.36	4.3	0.138
		O–O	2.51	4.0	0.083
		M–O	2.85	2.4	0.141
		P–P	2.92	1.9	0.097
$(CaO)_{0.445}(P_2O_5)_{0.445}(Na_2O)_{0.08}(Al_2O_3)_{0.03}$	2.7620(3)	P–NBO	1.50	2.2	0.032
		P–BO	1.60	1.5	0.044
		Al–O	1.73	2.2	0.025
		Al–O	1.82	1.8	0.057
		Al–O	1.92	4.5	0.066
		M–O	2.36	5.0	0.117
		O–O	2.51	3.5	0.072
		M–O	2.75	2.7	0.148
		P–P	2.96	1.7	0.097
$(CaO)_{0.445}(P_2O_5)_{0.445}(Na_2O)_{0.06}(Al_2O_3)_{0.05}$	2.7585(5)	P–NBO	1.50	2.2	0.034
		P–BO	1.60	1.4	0.043
		Al–O	1.71	1.7	0.040
		Al–O	1.82	1.6	0.047
		Al–O	1.91	3.4	0.092
		M–O	2.34	4.1	0.103
		O–O	2.50	3.4	0.069
		M–O	2.64	2.9	0.103
		P–P	2.91	1.8	0.073
$(CaO)_{0.445}(P_2O_5)_{0.445}(Na_2O)_{0.03}(Al_2O_3)_{0.08}$	2.7466(6)	P–NBO	1.50	2.3	0.034
		P–BO	1.60	1.2	0.041
		Al–O	1.71	2.3	0.053
		Al–O	1.80	1.7	0.019
		Al–O	1.93	2.3	0.050
		M–O	2.35	4.1	0.120
		O–O	2.51	3.3	0.072
		M–O	2.68	2.9	0.185
		P–P	2.93	1.4	0.096

aluminium remained relatively unaffected by the changing aluminium concentration.

IV. DISCUSSION

Phosphate glasses close to the metaphosphate composition have structures based upon interconnected PO_4^{3-} tetrahedral units.[36] These phosphate groups are joined to each other via bridging oxygen atoms (BOs). The remaining oxygen atoms in the phosphate groups are classified as non-bridging (NBOs) and coordinate to the cations present in the structure. Thus, the negatively charged interconnected phosphate units are held together by electrostatic forces that result from the cations present. Predictions concerning the phosphate connec-

TABLE II. NMR interaction parameters (isotropic chemical shift (δ_{iso}), quadrapole coupling constant (C_Q), and quadrapole asymmetry parameter (η)) and relative intensities obtained from the simulation of ^{27}Al MAS NMR data acquired at 9.4 and 14.1 T. The errors are identified within the table.

	Isotropic shift (ppm) ±1 ppm	C_Q centre (MHz) ±0.5	C_Q width ±0.6	η	Int (%)	Environment
$(CaO)_{0.445}(P_2O_5)_{0.445}(Na_2O)_{0.08}(Al_2O_3)_{0.03}$	42.6	4.3	4.1	0.1	24	AlO_4
	12.2	4.3	4.1	0.1	22	AlO_5
	− 10.5	4.5	4.1	0.1	54	AlO_6
$(CaO)_{0.445}(P_2O_5)_{0.445}(Na_2O)_{0.06}(Al_2O_3)_{0.05}$	46	5.9	3	0.1	31	AlO_4
	17.3	6.75	3	0.1	26	AlO_5
	− 9.2	5.1	3.3	0.1	43	AlO_6
$(CaO)_{0.445}(P_2O_5)_{0.445}(Na_2O)_{0.03}(Al_2O_3)_{0.08}$	41.5	0.7	0.1	0.1	9	Impurity
	44.8	5.8	3	0.1	34	AlO_4
	17.3	6.4	3	0.1	26	AlO_5
	− 8.2	5.3	3.3	0.1	31	AlO_6

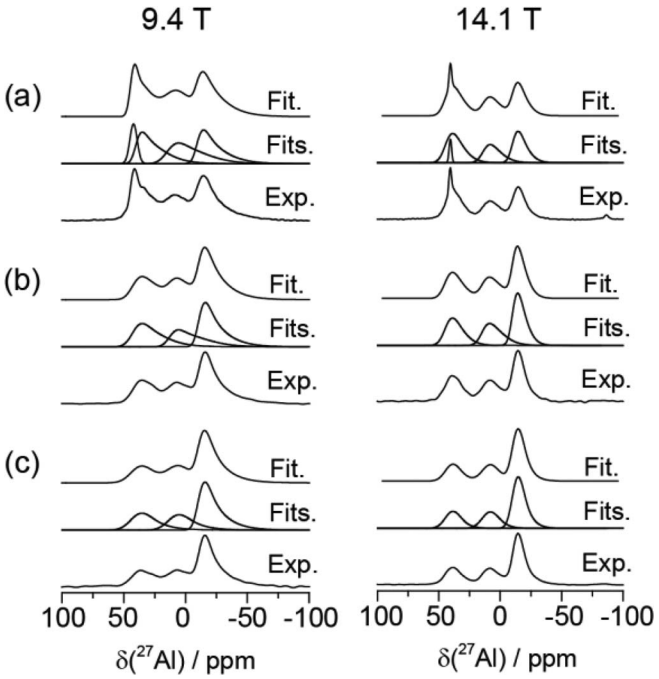

FIG. 5. ^{27}Al MAS NMR data acquired at 9.4 and 14.1T (ν_r = 20kHz) for the glass series $(Al_2O_3)_x(Na_2O)_{0.11-x}(CaO)_{0.445}(P_2O_5)_{0.445}$ with increasing Al concentration of (a) x = 0.03, (b) x = 0.05, and (c) x = 0.08. Each spectrum is deconvoluted into three individual resonances assigned to 4-, 5-, and 6- coordinate aluminium, and the self-consistency of the simulations between the two external magnetic field constrains the resultant NMR interaction parameters (δ_{iso}, C_Q, η) for optimal accuracy.

tivity can be made from the O/P ratio in glass composition.[36] Metaphosphate glasses are characterised by an O/P ratio of 3 and have structures consisting of rings and infinite chains of PO_4^{3-} tetrahedral. The glasses studied here have O/P ratios of 3.12, 3.19, 3.24, and 3.30 for the 0, 3, 5, and 8 mol. % Al_2O_3 samples, respectively. These fall in the range between the metaphosphate (PO_3^-) with composition P/O = 3.0 and pyrophosphate ($P_2O_7^{4-}$) with composition O/P = 3.5.[36] Since glasses of the latter composition have structures containing phosphate dimers, the glasses studied here are expected to have structures containing rings and shorter phosphate chains with the presence of only two types of phosphate species, i.e., $-PO_2^-$− middle groups and $-PO_3^{2-}$ chain-terminating end groups. The suitability of this proposed model to describe these samples can be gauged by calculating the expected P-BO, P-NBO, and P-P coordination numbers from the composition and comparing with those in Table I from the neutron diffraction data. The P-BO coordination number (N_{BO}) is given by

$$N_{BO} = 8 - 2(O/P). \quad (6)$$

Since each phosphorus atom is surrounded by four oxygen atoms in the PO_4^{3-}, the P-NBO coordination number (N_{NBO}) is simply $4 - N_{BO}$. Furthermore, since each bridging oxygen connects to another PO_4^{3-} unit, the P-P coordination number (N_{PP}) is equal to N_{BO}. The N_{BO} values calculated here on the basis of composition are 1.8, 1.6, 1.5, and 1.4 for the 0, 3, 5, and 8 mol. % Al_2O_3 samples, respectively, agree well with their respective experimentally determined values of 1.6 ± 0.2, 1.5 ± 0.2, 1.4 ± 0.2, and 1.2 ± 0.2. Similar agreement is observed between the calculated N_{NBO} values of 2.2, 2.4, 2.5, and 2.6 and their respective experimentally determined values of 2.2 ± 0.3, 2.2 ± 0.3, 2.2 ± 0.3, and 2.3 ± 0.3 for the 0, 3, 5, and 8 mol. % Al_2O_3 samples, respectively. Finally, the calculated N_{PP} values of 1.8, 1.6, 1.5, and 1.4 for the 0, 3, 5, and 8 mol. % Al_2O_3 samples, respectively, exhibit broad agreement with their respective experimentally determined values of 1.9 ± 0.2, 1.7 ± 0.2, 1.8 ± 0.2, and 1.4 ± 0.2. Considering these results as a whole, it can be concluded that the phosphate network that forms the backbone of the structure of the glasses is close to that expected on the basis of glass composition with the phosphorus present as both $-PO_2^-$− middle groups and $-PO_3^{2-}$ chain-terminating end groups. The proportion of $-PO_3^{2-}$ groups increases with Al_2O_3 content.

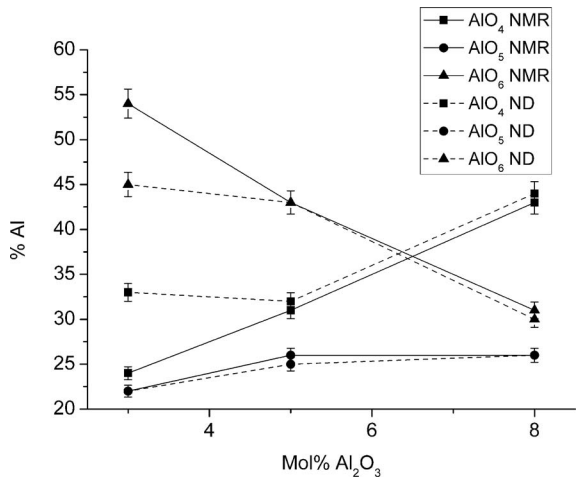

FIG. 6. Relative concentration of 4-, 5-, and 6-fold aluminium coordination environments as determined by neutron diffraction and ^{27}Al MAS-NMR spectroscopy. The format for the legend is such that AlO_4 ND refers to the concentration of 4-fold aluminium determined from the neutron diffraction data and AlO_5 NMR refers to the concentration of 5-fold aluminium determined from the ^{27}Al NMR data.

Of particular interest here is the coordination environment of the aluminium because this changes significantly as a function of Al_2O_3 content as does the measured density of the glasses. As shown in Figure 1, an initial increase in density is observed with the small addition of aluminium. This increase is as anticipated due to aluminium being a more massive atom than sodium. Indeed, a simplistic weighted sum of the components (using sodium phosphate, calcium phosphate, and aluminium phosphate in appropriate amounts) indicates that the density should continue to increase monotonically with the aluminium concentration. Subsequent increase in the aluminium concentration is, however, associated with an observed decrease in density, which is counter-intuitive. This density trend can be rationalized by considering the changes to the aluminium coordination environment as a function of Al_2O_3 content, which can readily be seen through the neutron diffraction results, with additional definitive assignments provided by the NMR results. These show that the initial small concentration of aluminium is largely 6-fold coordinated, although with a small amount of 4- and 5-fold coordinated aluminium present, whereas the samples

with larger concentrations of aluminium tend to be dominated by 4-fold coordinated sites with a reduced 6-fold coordination. The proportion of 5-fold coordinated aluminium seems to remain constant throughout the composition series. The effect that changing aluminium environment has on density can be understood by examining the density of crystals containing aluminium tetrahedrally or octahedrally coordinated by oxygen. The mineral Berlinite, $Al(PO_4)$, which contains aluminium in 4-fold sites has a density of 2.63 g/cm^3.[32,33] The mineral $NaAl(P_2O_7)$ contains 6-fold coordinated aluminium and has a density of 2.87g/cm^3.[34] By considering $NaAl(P_2O_7)$ as a one-to-one mixture of $Na(PO_3)$ and $Al(PO_4)$ and assuming that its density approximates to the average of the densities of these two compounds, an estimate of the density of $Al(PO_4)$ if it had a structure that consisted of 6-fold coordinated aluminium can be obtained. Taking the density of $Na(PO_3)$ as 2.60 g/cm^3,[27–31] a value of 3.14 g/cm^3 for $Al(PO_4)$ containing octahedrally coordinated aluminium is obtained, which is significantly higher than 2.63 g/cm^3 for the same compound containing tetrahedrally coordinated aluminium. Although this density of 3.14 g/cm^3 for 6-fold $Al(PO_4)$ is only a rough estimate, further evidence for a correlation between aluminium coordination number and density can be found by looking at the high pressure phase of Berlinite.[37,38] This phase contains only 5- and 6-fold aluminium reinforcing the correlation between higher density and higher coordination numbers. Thus, the likely explanation for the observed trend in the densities of the aluminium containing glasses is the changing local environment around the aluminium as the concentration of Al_2O_3 goes up; a similar effect is seen in the more complex Na_2O-Al_2O_3-TiO_2-P_2O_5 glass.[3]

The observed trend towards lower aluminium coordination number with increasing Al_2O_3 content is echoed by the results of previous studies[17,20,39] where a correlation between O/P ratio and average aluminium coordination number was observed. As O/P increased from 3 (metaphosphate) to >3.5 (pyrophosphate), the dominant Al coordination number changed from 6 to 4 in order to maintain the network charge balance.[39] Furthermore, changes in network connectivity observed in this study help explain the trend seen in the bioactivity observed elsewhere for glasses of the same composition.[9] Manupriya and co-workers[9] demonstrated that a decrease in dissolution rate with increasing aluminium content coincided with a decrease in bioactivity. It is known that the release rates of Ca^{2+} and PO_4^{3-} from biomaterials correlate with bioactivity[40] because the release of these ions into the surrounding solution as the glass degrades results in super-saturation of calcium and phosphate which favours apatite formation.[41,42] Consistent with the established structural models for phosphate based glass,[36] the neutron diffraction results presented here show that increasing the aluminium content of these glasses reduces the number of P-O-P bonds and reduces the connectivity of the phosphate network. Given that P-O-P bonds are readily hydrolysed in water and that higher field strength cations form stronger bonds between the phosphate chains in phosphate based glasses,[17] it follows that replacing Na^+ with Al^{3+} reduces dissolution rates resulting in lower bioactivity.

V. CONCLUSIONS

The neutron diffraction results demonstrate that the phosphate network forming the backbone of the structure of these Al_2O_3-Na_2O-CaO-P_2O_5 glasses is close to that expected on the basis of glass composition with the phosphorus present as both $-PO_2^-$– middle groups and $-PO_3^{2-}$ chain-terminating end groups. The proportion of $-PO_3^{2-}$ groups increases with Al_2O_3 content.

The observed variation in density with aluminium content can be related to the local environment of the aluminium atoms. Initially, with low concentrations of aluminium, 6-fold coordination of the aluminium environment is predominant. At higher aluminium concentrations the local aluminium environment is mainly 4-fold coordinated. There is some aluminium found in 5-fold coordination, but this amount appears to remain unaffected by the concentration of aluminium present.

ACKNOWLEDGMENTS

We wish to acknowledge funding from the EPSRC (EP/F021011/1), support and beam time from STFC, and the use of the EPSRC funded Chemical Database Service at Daresbury. J.V.H. acknowledges the continued funding of the 400 and 600 MHz solid state NMR instrumentation at Warwick used in this research as facilitated by EPSRC, the University of Warwick, and partial funding through Birmingham Science City Advanced Materials Projects 1 and 2 supported by Advantage West Midlands (AWM) and the European Regional Development Fund (ERDF).

[1] K. M. Weatherall, D. M. Pickup, R. J. Newport, and G. Mountjoy, J. Phys.: Condens. Matter **21**, 035109 (2009).
[2] E. A. Abou Neel, W. Chrzanowski, S. P. Valappil, L. A. O'Dell, D. M. Pickup, M. E. Smith, R. J. Newport, and J. C. Knowles, J. Non-Cryst. Solids **355**, 991 (2009).
[3] B. Tiwari, V. Sudarsan, A. Dixit, and G. P. Kothiyal, J. Am. Ceram. Soc. **94**, 1440 (2011).
[4] J. H. Campbell and T. I. Suratwala, J. Non-Cryst. Solids **263–264**, 318 (2000).
[5] I. Abrahmans, K. Franks, G. E. Hawkes, G. Philippou, J. C. Knowles, P. Bodart, and T. Nunes, J. Mater. Chem. **7**, 1573 (1997).
[6] *Biomaterials, Artificial Organs and Tissue Engineering*, edited by L. L. Hench and J. R. Jones (Woodhead Publishing Limited, Cambridge, 2005).
[7] I. Ahmed, M. Lewis, I. Olsen, and J. C. Knowles, Biomaterials **25**, 491 (2004).
[8] A. A. El-Kheshen, F. A. Khaliafa, E. A. Saad, and R. L. Elwan, Ceram. Int. **34**, 1667 (2008).
[9] K. S. Thind Manupriya, K. Singh, G. Sharma, and V. Rajendran, Phys. Status Solidi A **206**, 1447 (2009).
[10] J. Schneider, S. L. Oliveira, L. A. O. Nunes, F. Bonk, and H. Panepucci, Inorg. Chem. **44**, 423 (2005).
[11] P. Hartmann, J. Vogel, U. Friedrich, and C. Jager, J. Non-Cryst. Solids **263–264**, 94 (2000).
[12] D. M. Pickup, P. Guerry, R. M. Moss, J. C. Knowles, M. E. Smith, and R. J. Newport, J. Mater. Chem. **17**, 4777 (2007).
[13] A. J. Parsons, I. Ahmed, C. D. Rudd, G. J. Cuello, E. Pellegrini, D. Richard, and M. R. Johnson, J. Phys.: Condens. Matter **22**, 485403 (2010).
[14] J. Schneider, S. L. Oliviera, L. A. O. Nunes, and H. Panepucci, J. Am. Ceram. Soc. **86**, 317 (2003).
[15] A. M. Marquez, J. Oviedo, J. F. Sanz, J. J. Benitez, and J. A. Odriozola, J. Phys. Chem. B **101**, 9510 (1997).
[16] C. J. Benmore, J. K. R. Weber, S. Sampath, J. Siewenie, J. Urquidi, and J. A. Tangeman, J. Phys.: Condens. Matter **15**, S2413 (2003).
[17] E. Metwalli, R. K. Brow, and F. S. Stover, J. Am. Ceram. Soc. **84**, 1025 (2001).

[18]A. Belkebir, J. Rocha, A. P. Esculcas, P. Berthet, B. Gilbert, Z. Gabelica, G. Llabres, F. Wijzen, and A. Rulmont, Spectrochim. Acta, Part A **55**, 1323 (1999).
[19]L. van Wullen, G. Tricot, and S. Wegner, Solid State Nucl. Magn. Reson. **32**, 44 (2007).
[20]J. M. Egan, R. M. Wenslow, and K. T. Mueller, J. Non-Cryst. Solids **261**, 115 (2000).
[21]A. C. Hannon, Nucl. Instrum. Methods Phys. Res. A **551**, 88 (2005).
[22]E. Lorch, J. Phys. C **2**, 229 (1969).
[23]P. H. Gaskell, *Materials Science and Technology*, edited by J. Zarzycki (VCH, Cambridge, 1991).
[24]R. M. Moss, E. A. Abou Neel, D. M. Pickup, H. L. Twyman, R. A. Martin, M. D. Henson, E. R. Barney, A. C. Hannon, J. C. Knowles, and R. J. Newport, J. Non-Cryst. Solids **356**, 1319 (2010).
[25]T. F. Kemp and M. E. Smith, Solid State Nucl. Magn. Reson. **35**, 243 (2009).
[26]D. A. Fletcher, R. F. McMeeking, and D. J. Parkin, Chem. Inf. Comput. Sci. **36**, 746 (1996).
[27]A. Immirzi and W. Porzio, Acta Crystallogr. Sect. B **38**, 2788 (1982).
[28]K. H. Jost, Acta Crystallogr. **16**, 640 (1963).
[29]K. H. Jost, Acta Crystallogr. **16**, 428 (1963).
[30]K. H. Jost, Acta Crystallogr. **14**, 844 (1961).
[31]A. McAdam, K. H. Jost, and B. Beagley, Acta Crystallogr., Sect. B **24**, 1621 (1968).
[32]B. P. Onac and H. S. Effenberger, Am. Mineral. **92**, 1998 (2007).
[33]P. Labeguerie, M. Harb, I. Baraille, and M. Rerat, Phys. Rev. B **81**, 045107 (2010).
[34]J. Alkemper, H. Paulus, and H. Fuess, Z. Kristallogr. **209**, 616 (1994).
[35]R. A. Martin, P. S. Salmon, D. L. Carrol, M. E. Smith, and A. C. Hannon, J. Phys.: Condens. Matter **20**, 115204 (2008).
[36]R. K. Brow, J. Non-Cryst. Solids **263**, 1 (2000).
[37]J. Pellicer-Porres, A. M. Saitta, A. Polian, J. P. Itie, and M. Hanfland, Nature Mater. **6**, 698 (2007).
[38]M. Kanzaki, X. Xue, S. Reibstein, E. Berryman, and S. Namgung, Acta Crystallogr., Sect. B **67**, 30 (2011).
[39]R. K. Brow, R. J. Kirkpatrick, and G. L. Turner, J. Am. Ceram. Soc. **76**, 919 (1993).
[40]R. G. Hill and D. S. Brauer, J. Non-Cryst. Solids. **357**, 3884 (2011).
[41]M. Mneimne, R. G. Hill, A. J. Bushby, and D. S. Brauer, Acta Biomater. **7**, 1827 (2011)
[42]D. S. Brauer, M. Mneimne, and R. G. Hill, J. Non-Cryst. Solids **357**, 3328 (2011).